Received: 24 August 2022 | Revised: 13 February 2023 | Accepted: 20 February 2023

DOI: 10.1002/psp4.12955

ARTICLE

Population pharmacokinetics of tenofovir given as either tenofovir disoproxil fumarate or tenofovir alafenamide in an African population

Aida N. Kawuma[1,2] | **Roeland E. Wasmann**[1] | **Phumla Sinxadi**[1] | **Simiso M. Sokhela**[3] | **Nomathemba Chandiwana**[3] | **Willem D. F. Venter**[3] | **Lubbe Wiesner**[1] | **Gary Maartens**[1] | **Paolo Denti**[1]

[1]Division of Clinical Pharmacology, Department of Medicine, University of Cape Town, Cape Town, South Africa

[2]Infectious Diseases Institute, Makerere University College of Health Sciences, Kampala, Uganda

[3]Ezintsha, Faculty of Health Sciences, University of the Witwatersrand, Johannesburg, South Africa

Correspondence
Aida N. Kawuma, Infectious Diseases Institute, Makerere University, Kampala, Uganda.
Email: akawuma@idi.co.ug

Abstract

Tenofovir disoproxil fumarate (TDF) and tenofovir alafenamide (TAF) are prodrugs of the nucleotide analogue tenofovir, which acts intracellularly to inhibit HIV replication. Whereas TDF converts to tenofovir in plasma and may cause kidney and bone toxicity, TAF mostly converts to tenofovir intracellularly, so it can be administered at lower doses. TAF leads to lower tenofovir plasma concentrations and lower toxicity, but there are limited data on its use in Africa. We used data from 41 South African adults living with HIV from the ADVANCE trial and described, with a joint model, the population pharmacokinetics of tenofovir given as TAF or TDF. The TDF was modeled to appear in plasma as tenofovir with a simple first-order process. Instead, two parallel pathways were used for a TAF dose: an estimated 32.4% quickly appeared as tenofovir into the systemic circulation with first-order absorption, whereas the rest was sequestered intracellularly and released into the systemic circulation as tenofovir slowly. Once in plasma (from either TAF or TDF), tenofovir disposition followed two-compartment kinetics and had a clearance of 44.7 L/h (40.2–49.5), for a typical 70-kg individual. This semimechanistic model describes the population pharmacokinetics of tenofovir when dosed as either TDF or TAF in an African population living with HIV and can be used as a tool for exposure prediction in patients, and to simulate alternative regimes to inform further clinical trials.

Study Highlights

WHAT IS THE CURRENT KNOWLEDGE ON THE TOPIC?

Tenofovir disoproxil fumarate (TDF), a tenofovir prodrug, is widely used for the treatment of HIV. It has been associated with kidney and bone toxicity. Tenofovir alafenamide (TAF) is a newer prodrug of tenofovir that mostly converts intracellularly and can therefore be dosed at lower strengths. It has been reported to have

fewer associated side effects compared to TDF. There are limited data on the use of TAF in low- and middle-income countries.

WHAT QUESTION DID THIS STUDY ADDRESS?

We aimed to characterize the population pharmacokinetics of tenofovir in a population of South African adults living with HIV. In particular, we focused on describing the differences between how TDF and TAF get absorbed, converted, and eventually appear in plasma as tenofovir.

WHAT DOES THIS STUDY ADD TO OUR KNOWLEDGE?

This study proposes a semimechanistic model describing the absorption of TDF and TAF and their appearance in plasma as tenofovir and its disposition in South Africans living with HIV.

HOW MIGHT THIS CHANGE CLINICAL PHARMACOLOGY OR TRANSLATIONAL SCIENCE?

There is interest in expanding the use of TAF in low- and middle-income countries, implying the need for further studies. This mechanistic model provides a framework that can be used to study and better understand the effect of drug–drug interactions, and pharmacogenetics' effect, or extrapolate to other populations or alternative dosing scenarios.

INTRODUCTION

Tenofovir is a nucleotide analogue that inhibits human immunodeficiency virus (HIV) replication. Because of its poor membrane permeability and low oral bioavailability, tenofovir is administered as a prodrug: either as tenofovir disoproxil fumarate (TDF) or tenofovir alafenamide (TAF). TDF or TAF are widely used in combination with other antiretroviral agents for the treatment of HIV because of their effective antiviral activity, favorable safety profile, and their availability within several fixed-dose co-formulated tablets.[1]

For their conversion to tenofovir, TDF and TAF undergo distinctly different processes, as portrayed in Figure 1. After oral administration, TDF is rapidly converted to tenofovir by esterase enzymes in the gut and plasma, leading to higher plasma concentrations of tenofovir relative to TAF.[2] Tenofovir is then taken into the cells and sequentially activated to tenofovir-diphosphate (TFV-DP).[3] On the other hand, TAF more efficiently delivers tenofovir to HIV-target cells because of its relative stability in plasma and its rapid absorption intracellularly. Consequently, in plasma, TAF has a short half-life of ~25 min and reaches undetected levels by about 4 to 6 h postdose.[4] Intracellularly, TAF is converted to tenofovir by cathepsin A and then activated to TFV-DP. This allows TAF to be given at a lower dose than TDF, leading to markedly lower levels of tenofovir in plasma, and, as a result, reduces off-target exposure. Higher tenofovir exposures when receiving TDF have been associated with an increased incidence of proximal tubular dysfunction, acute kidney injury, chronic kidney disease, and reduced bone mineral density.[5–7] The World Health Organization HIV treatment guidelines recommend the use of TAF (instead of TDF) for adults with established osteoporosis and/or impaired kidney function.

Tenofovir is eliminated renally by a combination of active tubular secretion and glomerular filtration. Tenofovir is not a substrate of cytochrome P450, P glycoprotein (P-gp) or multidrug resistance protein type 2.[8] Conversely, TAF is a substrate of P-gp and human breast cancer resistance protein and the pharmacokinetic boosters, ritonavir and cobicistat, which inhibit intestinal P-gp, can increase TAF plasma concentrations about twofold.[9]

The ADVANCE study (NCT03122262) carried out in South Africa showed that a regimen of TAF, dolutegravir, and emtricitabine was safe and well-tolerated in a South African population living with HIV.[10] The objective of our analysis was to develop a single population pharmacokinetic model that characterizes tenofovir appearance in plasma and disposition whether it is administered as TAF or TDF in South Africans living with HIV.

METHODS

Study population and procedures

Tenofovir concentration-time data were available from a pharmacokinetic substudy nested within the ADVANCE study, an open-label, phase III, randomized noninferiority trial comparing three first-line antiretroviral regimens in

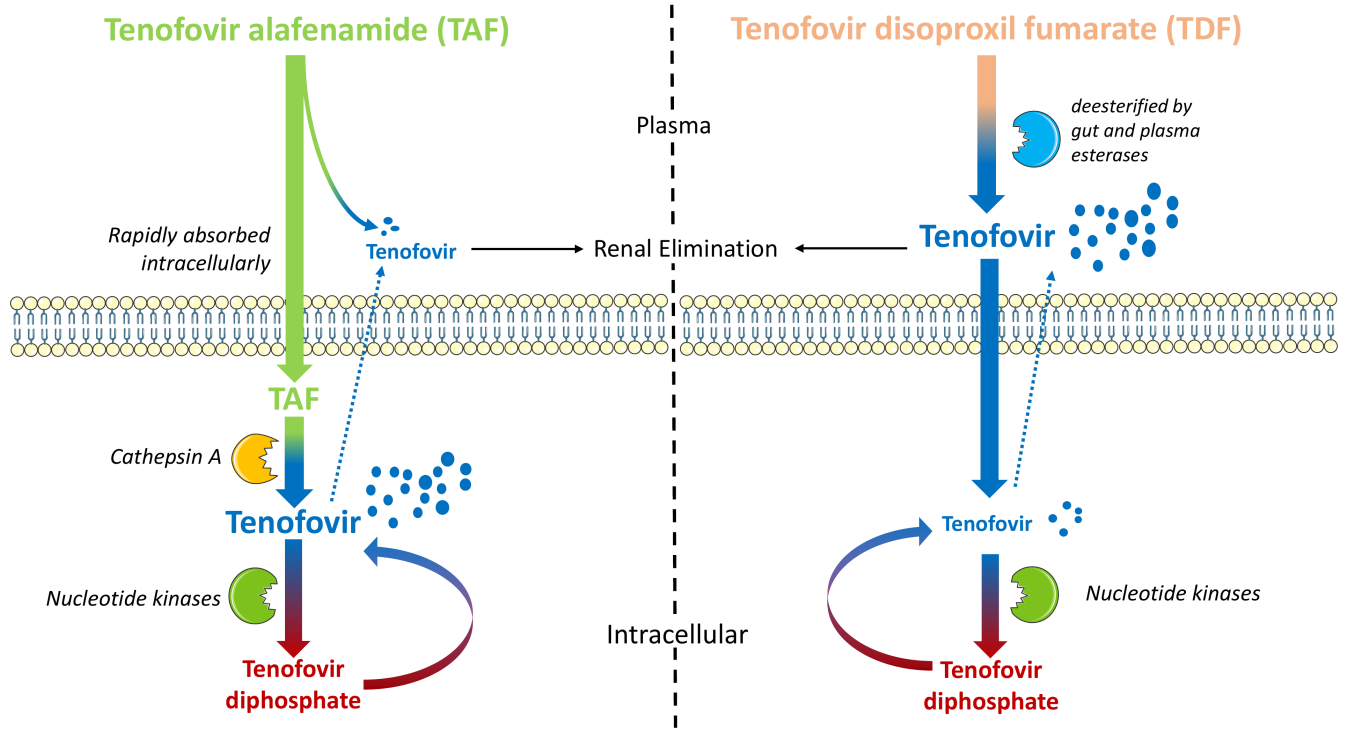

FIGURE 1 Schematic of the conversion of TDF and TAF to tenofovir. TAF is rapidly absorbed intracellularly where it is sequentially converted to TFV-DP. The TFV-DP then degrades to tenofovir intracellularly, which seeps back into the plasma. TDF is mostly converted to tenofovir in the plasma and then tenofovir is absorbed intracellularly where it undergoes sequential conversion to TFV-DP. Overall, when given as TDF, tenofovir in the plasma is more than 10-fold higher than when TAF is administered. TAF, tenofovir alafenamide; TDF, tenofovir disoproxil fumarate; TFV-DP, tenofovir-diphosphate.

treatment-naïve adults with HIV initiating antiretroviral therapy in South Africa. Full study procedures have been reported previously.[10] Briefly, the efficacy and safety of two prodrugs of tenofovir, TAF and TDF both combined with emtricitabine, were evaluated with dolutegravir versus a TDF-emtricitabine-efavirenz regimen (the standard of care at the time). Drugs in the three arms were dosed as dolutegravir (50 mg; ViiV Healthcare) plus co-formulated TAF (25 mg)/emtricitabine (200 mg; Gilead Sciences); dolutegravir (50 mg; ViiV Healthcare) plus generic versions of co-formulated TDF (300 mg)/emtricitabine (200 mg); and co-formulated TDF (300 mg)/emtricitabine (200 mg)/efavirenz (600 mg) from generic manufacturers. Rich pharmacokinetic sampling was performed in a subset of participants in the dolutegravir arms after at least 48 weeks of treatment. Samples were taken predose and 1, 2, 4, 6, 8, and 24 h postdose.

Analytical assay

Plasma tenofovir concentrations were determined with a validated liquid chromatography–tandem mass spectrometry assay developed at the Division of Clinical Pharmacology, University of Cape Town. The method utilized plasma protein precipitation, followed by high-performance liquid chromatography with tandem mass spectrometry detection. Chromatographic separation was achieved on a Waters Atlantis T3 column (2.1 mm × 100 mm, 3 μm) with a total runtime of 6 min. A Sciex 5500 Qtrap mass spectrometer at unit resolution in the multiple reaction monitoring mode was used to monitor the transition of the protonated precursor ions, 288.1 and 294.1 to the product ions 176.1 and 182.1 for tenofovir and tenofovir-d6 (internal standard), respectively. Electrospray ionization was used for ion production. The calibration curve fitted a quadratic (weighted by 1/concentration) regression based on peak area ratios over the range of 0.500 to 300 ng/mL. The combined accuracy (%Nom) of the limit of quantification, low, medium, and high-quality controls (three validation batches, $N = 18$) were between 93.8% and 103.8%, with precision (percent coefficient of variation) less than 13%.

Population pharmacokinetic modeling

Data were analyzed by non-linear mixed-effects modeling with NONMEM (version 7.5.0) using the first-order conditional estimation method with interaction.

Pearl-speaks-NONMEM (PsN) version 5.2.6, R version 3.6.1, and Pirana version 2.9.7. were used to assist model development.[11] Using their molecular weights, the dose of TDF and TAF in mg was converted to tenofovir (molecular weight = 287.2 g/mol) amounts in mg; 300 mg of TDF (molecular weight = 635.5 g/mol) provided 136 mg of tenofovir, whereas 25 mg of TAF (molecular weight = 476.5 g/mol) provided 15 mg of tenofovir.

We first modeled the kinetics of tenofovir when given as TDF, and explored one- and two-compartment disposition models with first-order elimination and absorption, with or without absorption lag time and transit compartments.[12] Afterward, we modeled tenofovir in the TAF arm and initially fixed the disposition parameters to what was observed for TDF. This was to reflect the fact that, once tenofovir appears in plasma, its kinetics will be the same irrespective of the prodrug used to administer it. We explored different semimechanistic models to describe how TAF appears as tenofovir in plasma. These included a model in which tenofovir absorption from TAF was described with two depot (absorption) compartments. One with a sequential zero-order infusion followed by a first-order absorption rate constant and the other described by only a first-order absorption rate constant. Whereas tenofovir from TDF was described by single first-order absorption with or without lag. In another model we tested, tenofovir from TAF was described by first-order absorption from two depot (absorption) compartments. One defined by a series of transit compartments and another described by a lag. Although tenofovir from TDF was described by single first-order absorption with or without lag.

Once the structure for TAF absorption and conversion to tenofovir was identified, both arms (TAF and TDF) were jointly fit in the same model and all parameter values were re-estimated. We included between-subject variability (BSV) and between-occasion variability (BOV) on disposition and absorption parameters respectively, assuming a log-normal distribution. For this analysis, an "occasion" was defined as a dose with its proceeding sample. For example, the unobserved dose the day before the pharmacokinetic visit (leading to the predose sample) was considered a separate occasion from the observed dose on the day of the pharmacokinetic visit (with its proceeding samples at 1, 2, 4, 6, 8, and 24 h postdose).

We tested error models with additive and/or proportional components to describe residual variability. The additive component of the error was constrained to be at least 20% of the lower limit of quantification (LLOQ). Allometry with either total body weight or fat-free mass (FFM)[13] was tested in the model and allometric exponents for clearance and volume were fixed to 0.75 and 1, respectively.[14] To discriminate between nested models, a decrease in the objective function value (OFV) of 3.84 was equivalent to model improvement at a significance level of $p < 0.05$, for one additional degree of freedom. In addition, model development was guided by the inspection of goodness-of-fit plots. We investigated the effect of age and baseline creatinine clearance on tenofovir's pharmacokinetic parameters. Covariates were assessed by stepwise inclusion ($\Delta OFV > 3.84$, $p < 0.05$) followed by backward elimination ($\Delta OFV > 6.63$, $p < 0.01$). Model performance was evaluated with a visual predictive check (VPC), and we used sampling importance resampling to generate the 95% confidence interval (95% CI) for parameter estimates.[15]

We used the final model to simulate steady-state estimates of the tenofovir area under the concentration-time curve ($AUC_{0\text{-}24h}$), for 1000 typical individuals with different representative weights. Estimates of $AUC_{0\text{-}24h}$ were obtained using the formula $AUC_{0\text{-}24h} = F_i \times Dose_i/CL_i$, where Dose represents TAF (25 or 10 mg) or TDF (300 mg). We compared the simulated $AUC_{0\text{-}24h}$ values (median and range) with previously reported AUC values from different studies.

RESULTS

Forty-one individuals in a 1:1 ratio (21 on TDF vs. 20 on TAF) provided 279 tenofovir concentrations. Median (interquartile range) of weight, age, and creatinine clearance (at screening) estimated by Cockcroft and Gault were 73.1 (67.2–85.2) kg, 31 (29–36) years, and 120 (96.0–140) mL/min respectively. There was no significant difference in weight, age, or creatinine clearance (at screening) between the TDF and TAF arms. Participant demographics are reported in Table 1. None of the samples had a concentration below the LLOQ.

A schematic illustrating the structure of the pharmacokinetic model is shown in Figure 2. A two-compartment disposition model ($\Delta OFV = -47$, $p < 0.001$ compared to one-compartment) best described the pharmacokinetics of tenofovir in plasma. Allometric scaling with weight described the effect of body size on disposition parameters and was applied to all clearance and volume parameters ($\Delta OFV = -18$ compared to no allometry). Compared to no allometry, scaling with FFM did not improve the model significantly ($\Delta OFV = -3.80$). For a typical individual of 70 kg, clearance was estimated at 44.7 (40.2–49.5) L/h. Adding creatinine clearance (collected at screening) as a covariate on clearance, did not improve the model significantly and neither did age. TDF was found to quickly appear as tenofovir in plasma with a first-order rate constant of 3.04 (2.11–3.88) h^{-1}. Instead, the release of tenofovir after TAF administration was described by two absorption pathways: a fraction available for immediate absorption into the systemic circulation ($Frac_{TAF\text{-}Fast}$) and a slow fraction ($Frac_{TAF\text{-}Slow}$) modeled as if it was first

TABLE 1 Participant demographics.

Characteristic	Median (interquartile range)		
	TDF Regimen (Plus, FTC-DTG) $n = 21$ (51.2%)	TAF Regimen (Plus, FTC-DTG) $n = 20$ (48.8%)	ALL ($n = 41$)
Sex, *n* (%) male/female	8 (38.1)/13 (69.1)	6 (30.0)/14 (70.0)	14 (34.1)/27 (65.9)
Age, years	34.0 (27, 40)	30.5 (29, 33.3)	31.0 (29.0, 36.0)
Weight, kg	74.3 (61.4, 89.1)	73 (68.3, 81.8)	73.1 (67.2, 85.2)
Height, cm	169 (162, 175)	165 (159, 171)	167 (161, 174)
Creatinine clearance at screening, mL/min[a]	115 (93, 145)	123 (106, 138)	120 (96.0, 140)

Abbreviations: DTG, dolutegravir; FTC, emtricitabine; TAF, tenofovir alafenamide; TDF, tenofovir disoproxil fumarate.

[a]Creatinine clearance was calculated by Cockcroft and Gault.

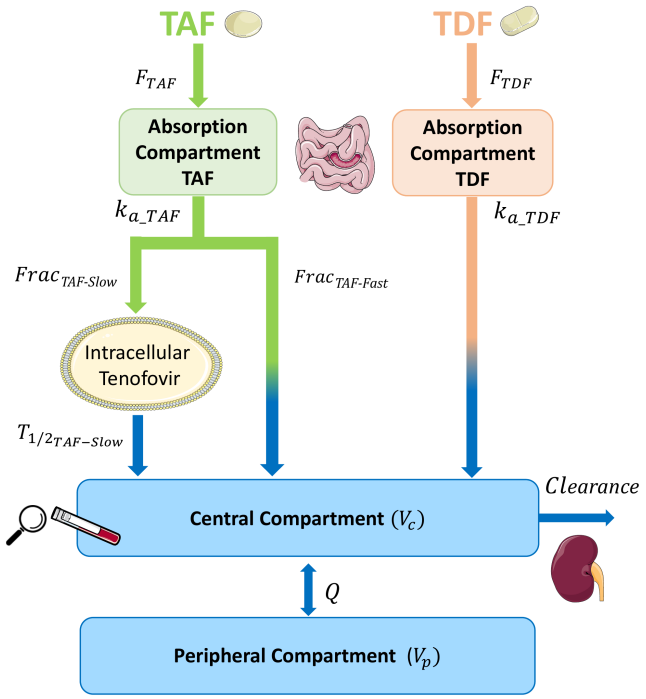

FIGURE 2 Schematic of the tenofovir structural model. Once administered, the dose of tenofovir given as TDF is absorbed into the central compartment. It then distributes to a peripheral compartment and is eliminated from the central compartment with first-order kinetics. When given as TAF, a fast fraction ($Frac_{TAF\text{-}Fast}$) is immediately absorbed into systemic circulation while a slow fraction ($Frac_{TAF\text{-}Slow}$) = (1 − F $Frac_{TAF\text{-}Fast}$) is first absorbed intracellularly and then slowly transitioned to the systemic circulation via a first-order process with a half-life in days ($t_{1/2\_TAF\text{-}Slow}$). CL, central clearance; K_a, absorption rate constant; Q, intercompartmental clearance; TAD, tenofovir disoproxil fumarate; TAF, tenofovir alafenamide; V_c, central volume of distribution; V_p, peripheral volume of distribution.

absorbed intracellularly into a reservoir and then slowly released as tenofovir to the systemic circulation. $Frac_{TAF\text{-}Fast}$ was estimated to be 32.4% (27.0–37.7) and to become plasma tenofovir with a first-order rate constant of 1.45 h^{-1} (0.924–2.60). The remaining $Frac_{TAF\text{-}Slow}$ appeared as tenofovir in the systemic circulation with a terminal half-life ($t_{½}$)$_{TAF\text{-}Slow}$, which was fixed to 6.8 days. This value was initially estimated from the data, but the parameter estimate was poorly identifiable. A likelihood profiling exercise revealed that values in the range of 5 to 60 days provided only small changes in terms of goodness-of-fit. For this reason, we decided to fix the parameter value to 6.8 days, which has been previously reported as the $t_{½}$ of intracellular TFV-DP decay.[16] Results of the sensitivity analysis for this $t_{½\_TAF\text{-}Slow}$ parameter are reported in Table S1 and Figure S4. The relative bioavailability of tenofovir when given as TAF, was estimated to be 82.2% (95% CI, 72.3–93.9). Within the TAF arm, the model did not support the estimation of any variability (BOV or BSV) on the bioavailability parameter. None of the other alternative models we tested during the model development process fit the observed data as well as the one we report here.

Final parameter estimates and their precision are presented in Table 2. A VPC stratified by the treatment arm (TDF vs. TAF) in Figure 3 shows that the final model described the observed data adequately, with the median, 5th, and 95th percentiles of the observed data falling within the 95% CI of the respective prediction. The raw data and goodness-of-fit plots are provided in the supplements (Figures S1 to S3).

A comparison of our simulated $AUC_{0\text{-}24h}$ values to those previously reported in three different studies is summarized in Table 3. Predominantly, the AUC values simulated with our model are in good agreement with those previously reported, even when other doses (TAF 10 mg) are simulated.

DISCUSSION

We developed a joint semimechanistic model that describes the population pharmacokinetics of tenofovir

TABLE 2 Final population parameter estimates for tenofovir.

Parameter description	Typical value (95% CI)[a]	Parameter variability (%CV)[b] (95% CI)[a]
CL (L/h)[c]	44.7 (40.2–49.5)	20.1 (16.1–24.7)[d]
V_c (L)[c]	378 (319–459)	
Q (L/h)[c]	157 (103–233)	
V_p (L)[c]	356 (298–438)	
F_{TDF} (·)	1—Fixed	23.9 (18.2–30.3)[e]
F_{TAF} (·)	0.822 (0.723–0.939)	
K_{a_TDF} (1/h)	3.04 (2.11–3.88)	114.5 (68.4–162)[e]
K_{a_TAF} (1/h)	1.45 (0.924–2.60)	66.3 (31.0–91.6)[e]
$t_{1/2\_TAF\text{-}Slow}$, days	6.83—Fixed	
$Frac_{TAF\text{-}Fast}$ (%)	32.4 (27.0–37.7)	
Proportional error (%)	11.9 (10.8–13.4)	
Additive error, mg/L	20% of LLOQ[f]—Fixed	

Abbreviations: %CV, coefficient of variation; CI, confidence interval; CL, clearance; K_a, absorption rate constant; LLOQ, lower limit of quantification; Q, inter-compartmental clearance; V_c, central volume of distribution; V_p, peripheral volume of distribution.

[a]The 95% CIs were obtained by Sampling importance resampling.

[b]Between-subject variability (BSV) and between-occasion variability (BOV) were assumed to be log-normally distributed and calculated by $\text{CV}\% = \sqrt{\omega^2} \cdot 100$.

[c]Allometric scaling with weight (for a reference individual of 70 kg) was used for the CL, Q, V_c, V_p, %CV, and K_a. The half-life of the first-order process by which tenofovir leaves the intracellular compartment to the central compartment ($t_{1/2\_TAF\text{-}Slow}$). Percentage of tenofovir that is immediately available for absorption into the systemic circulation ($Frac_{TAF\text{-}Fast}$).

[d]Between-subject variability.

[e]Between-occasion variability.

[f]The LLOQ was 0.0005 mg/L.

after TAF and TDF administration. A key strength of our model is the fact that the model uses the same disposition parameters (and therefore clearance) for tenofovir in plasma, regardless of the prodrug used to administer it. In addition, we describe separate absorption processes for TDF and TAF. TDF quickly appears in plasma as tenofovir, whereas, after TAF administration, the absorption of tenofovir is described using two pathways, as illustrated in Figure 2. With this implementation, we aim to mimic the fact that once absorbed, most TAF is rapidly taken up intracellularly and then subsequently converted to TFV-DP. The TFV-DP is then degraded intracellularly to tenofovir, which then seeps back into the plasma.

Several population pharmacokinetic models for tenofovir have been reported previously, the majority when dosed as TDF.[17–23] An exception is the model by Greene et al.,[24] in which the authors describe tenofovir pharmacokinetics after both TDF and TAF administration in men living with HIV in the United States. However, they use two separate models, one when TDF is administered and another when TAF is administered. As such, they reported two separate clearance values (with a ~10-fold difference). Although the models sufficiently described their observed data, the use of two separate disposition models is a limitation of their approach and is difficult to justify from a mechanistic perspective. Once tenofovir has reached the plasma, it should distribute and be eliminated in the same manner, regardless of the prodrug from whence it came. The lack of a mechanistic interpretation for the models may imply that, while suited to describe the data on which they were developed, they may not be reliable to extrapolate to new dosing scenarios, or when predicting the effect of drug–drug interactions.

Ruane et al. showed that tenofovir had a $t_{½}$ of 14.86 h when given as TDF, whereas this value increased to 40.19 h when given as TAF, thus demonstrating that tenofovir disappears from plasma more slowly when the TAF prodrug is administered.[4] In our approach, we postulate that the observed difference in the $t_{½}$ of tenofovir when dosed as TAF versus TDF must be explained by the different mechanisms with which tenofovir from the two prodrugs eventually appears in plasma, and not by the distribution and elimination of tenofovir. In the case of TAF, our model assumes that a large fraction of the prodrug is absorbed into a reservoir compartment outside of the plasma. Although this reservoir may consist of many cell types, we believe it largely represents the peripheral blood mononuclear cells (PBMCs),

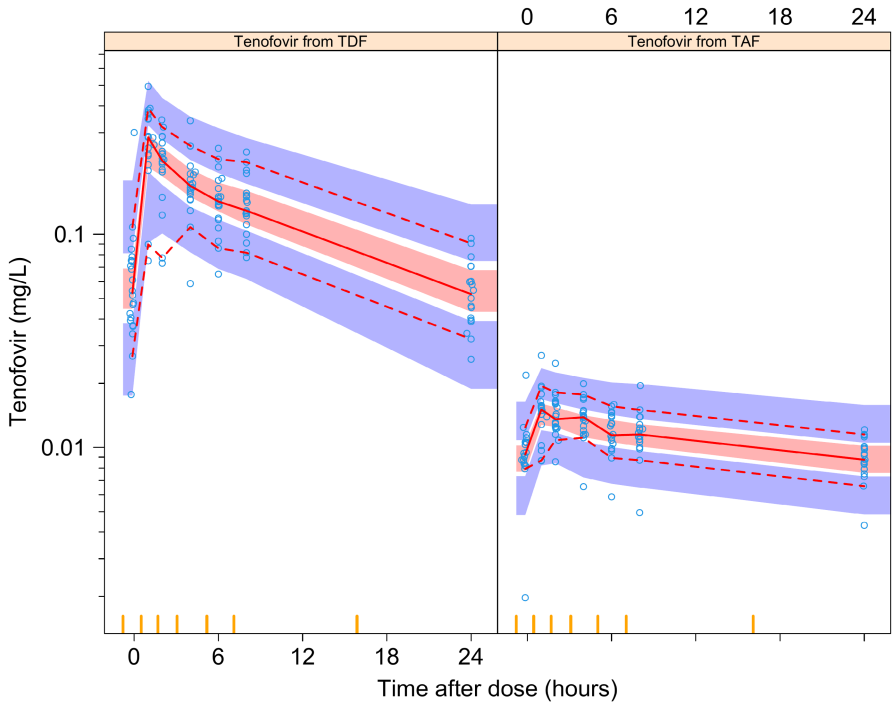

FIGURE 3 Visual predictive check of the final model. Blue circles represent observed plasma concentrations. The solid line in the middle represents the median observed concentration, and the broken lines below and above it represents the 5th and 95th percentiles of the observed concentrations, respectively. The shaded areas around each line represent the 95% confidence interval for the same percentiles based on simulations with the model. TAD, tenofovir disoproxil fumarate; TAF, tenofovir alafenamide.

TABLE 3 Comparison of previously reported AUC values to simulated AUC values derived with the final model.[a]

		Tenofovir $AUC_{0\text{-}24}$ (ng·h/mL) median (range)	
Study/Simulation characteristics	**Study**	**Received TDF**	**Received TAF**
Median weight (range) = 73.1 (67.2, 85.2) TDF dose = 300 mg TAF dose = 25 mg	Observed (this study, Reference)	3022 (1164, 5243)	267.1 (122.7, 457.1)
Typical weight = 77 kg TDF dose = 300 mg TAF dose = 25 mg	Model simulations	2795 (1393, 6095)	253.6 (141.5, 470.5)
	Reported by Thurman et al.[30,b]	2943 (1371, 4014), *n = 25*	294 (178, 671), *n = 24*
Typical weight = 77 kg TAF dose = 10 mg	Model simulations	–	101.6 (54.80, 208.2)
	Reported by Thurman et al.[30,b]	NA	101 (21, 167), *n = 26*
Typical weight = 78.7 kg TAF dose = 25 mg	Model simulations	–	259.8 (20.86)
	Reported by Begley et al.[31,c,d]	NA	238 (14.0), *n = 17*[e,f]
Typical weight = 74.3 kg TAF dose = 10 mg	Model simulations	–	108.6 (20.68)
	Reported by Begley et al.[31,c,d]	NA	115 (16.9), *n = 10*[e,g]
Median weight = 52 kg TDF dose = 300 mg	Model simulations	3761 (2022, 6997)	–
	Reported by Cressey et al.[2,c,h]	2526 (1881, 3392), *n = 9*	NA

Abbreviations: AUC, area under the curve; TAF, tenofovir alafenamide; TDF, tenofovir disoproxil fumarate; NA, not applicable.

[a]Model simulations are based on 1000 runs of a single typical individual of the weight and dose specified per study excluding between-occasion variability on absorption parameters.

[b]In Thurman et al., body size was reported as body mass index (BMI; kg/m^2), with mean values of 26.7, 27.0 and 26.8 kg/m^2 for the 10 mg TAF arm, 25 mg TAF arm, and 300 mg TDF arm, respectively. Therefore, for purposes of simulation and ease of comparison, we impute a typical weight of 77 kg for all the three arms (this translates to a BMI of 27 at a height of 169 cm with height).

[c]Healthy volunteers.

[d]This study did not have a TDF arm and therefore, no tenofovir concentrations from TDF were simulated for the typical weight.

[e]Data are reported as mean (percent coefficient of variation).

[f]TAF was administered alone (without any accompanying drugs), and data reported is AUC_{tau} (ng. h/mL).

[g]TAF was administered with dolutegravir and emtricitabine and the data reported is AUC_{inf} (ng. h/mL).

[h]This study did not have a TAF arm and therefore, no tenofovir concentrations from TAF were simulated for the typical weight.

into which the majority of tenofovir is sequestered when given as TAF. It is some of this intracellular tenofovir that then leaks back out into the plasma. We postulate that the available tenofovir intracellularly (70%) is phosphorylated to TFV-DP and is only released to transition back into the plasma after the diphosphate decays back to tenofovir. Hence, the half-life of the transition of tenofovir from the intracellular compartment to the plasma is limited mostly by the rate of diphosphate conversion.

This is in line with results by Lee et al.,[25] who showed that compared to TDF, TAF preferentially concentrates in PBMCs as opposed to red blood cells. Interestingly, for the TAF arm, the tenofovir concentration-time profiles (in Figure S3 and the VPC in Figure 3) show that after an initial peak at about 1 h postdose, there is a secondary peak at about 4 h postdose. This secondary peak could be caused by intracellular TAF being converted to tenofovir, which then leaks out of the cells to the plasma.

Like previous reports, we describe a two-compartment disposition model with first-order elimination for tenofovir. Our values of clearance (central and intercompartmental), and volume of distribution (central and peripheral) are all within the range of previous reports.[17–19,26–28] Our sampling schedule allowed for adequate estimation of two separate first-order absorption rate constants for the TAF ($1.45\,h^{-1}$) and TDF ($3.04\,h^{-1}$) arms. These values are in line with previous reports, with one publication reporting a value (median 95% CI) of 1.06 (0.62–1.86) h^{-1},[29] and another as high as 4.7 (1.46–128.15) h^{-1}.[18]

One limitation of our model is that we were not able to quantify the effect of renal function on tenofovir clearance, which has previously been reported to be significant.[3] This could be due to the narrow distribution of values of creatinine clearance in our cohort (with a median and interquartile range of 120 and 96.0–140 mL/min, respectively), and possibly the fact that measurements of creatinine were not available at the time of sampling for drug concentration. However, because the disposition of tenofovir in our model is compatible with previous reports, one can speculate that results of the effect of renal function on clearance could be carried across.

A major limitation is that we do not have plasma TAF concentrations and neither do we have tenofovir concentrations in PBMCs. We only have plasma tenofovir concentrations and, therefore, we validate our predictions in terms of the way tenofovir appears in plasma. However, TAF is very short-lived in plasma and usually reaches undetectable levels in plasma 4 to 6 h postdose. Therefore, even though we did not observe this in our study, our model is consistent with the literature.

In conclusion, the semimechanistic model we developed adequately described tenofovir concentrations in a cohort of South African adults living with HIV. This model plausibly describes the differences observed between the conversion of TDF and TAF to tenofovir and the resulting different exposures in plasma. The model should foster further investigation of the use of TAF as it offers a tool for investigating drug–drug interactions, exposure predictions in patients, and for simulation of alternative dosing regimens and for further clinical trials that may increasingly involve the use of TAF in place of TDF for the treatment of HIV in resource-constrained settings. Considering that there are still limited published pharmacokinetic data on TAF in low- and middle-income countries, especially in persons co-infected with tuberculosis, children, and pregnant women, more studies are needed to further elucidate the dosing of this drug in such scenarios and compare it with TDF. We believe a semimechanistic approach, such as the one that we suggest here, is going to be essential to correctly interpret the results from these studies.

AUTHOR CONTRIBUTIONS

A.N.K., R.E.W., G.M., and P.D. wrote the manuscript. P.S. and W.D.F.V. designed the research. S.M.S. and N.C. performed the research. A.N.K., R.W., and P.D. analyzed the data. L.W. contributed new reagents/analytical tools.

ACKNOWLEDGMENTS

The authors wish to thank the research staff and study participants who took part in the ADVANCE trial. Computations were performed using facilities provided by the University of Cape Town's ICTS High-Performance Computing team: http://hpc.uct.ac.za.

FUNDING INFORMATION

The ADVANCE study is funded by Unitaid, US Agency for International Development (USAID), the South African Medical Research Council, and ViiV Healthcare, with investigational product provided by ViiV Healthcare and Gilead Sciences. This work was supported in part by the National Research Foundation of South Africa (Grant Number 113368, awarded to G.M.). A.N.K. was supported by a doctoral training grant from Pharmacometrics Africa NPC. P.S. was supported in part by the South African Medical Research Council under a self-initiated research grant and the National Research Foundation (Thuthuka UID113983 and the Black Academic Advancement Programme UID120647). The laboratory at the University of Cape Town was supported by the National Institute of Allergy and Infectious Diseases (NIAID) of the National Institutes of Health (Award nos. UM1 AI068634, UM1 AI068636, and UM1 AI106701). The content is solely the responsibility of the authors and does not necessarily represent the official views of the sponsors.

CONFLICT OF INTEREST STATEMENT

Through their institution, P.S., S.S., N.C., and W.D.F.V. received research funding and drug donation for the ADVANCE trial from ViiV Healthcare and Gilead Sciences. All other authors declared no competing interests for this work.

ORCID

Aida N. Kawuma https://orcid.org/0000-0001-7975-0178
Roeland E. Wasmann https://orcid.org/0000-0002-5769-8150
Phumla Sinxadi https://orcid.org/0000-0002-1312-3523
Simiso M. Sokhela https://orcid.org/0000-0002-2707-1533
Nomathemba Chandiwana https://orcid.org/0000-0001-7866-2651
Willem D. F. Venter https://orcid.org/0000-0002-4157-732X
Lubbe Wiesner https://orcid.org/0000-0002-9070-8699
Gary Maartens https://orcid.org/0000-0003-3080-6606
Paolo Denti https://orcid.org/0000-0001-7494-079X

REFERENCES

1. Estrella MM, Moosa MR, Nachega JB. Editorial commentary: risks and benefits of Tenofovir in the context of kidney dysfunction in sub-Saharan Africa. *Clin Infect Dis*. 2014;58:1481-1483.
2. Cressey TR, Siriprakaisil O, Kubiak RW, et al. Plasma pharmacokinetics and urinary excretion of tenofovir following cessation in adults with controlled levels of adherence to tenofovir disoproxil fumarate. *Int J Infect Dis*. 2020;97:365-370.
3. Kearney BP, Flaherty JF, Shah J. Tenofovir disoproxil fumarate: clinical pharmacology and pharmacokinetics. *Clin Pharmacokinet*. 2004;43:595-612.
4. Ruane PJ, DeJesus E, Berger D, et al. Antiviral activity, safety, and pharmacokinetics/pharmacodynamics of tenofovir alafenamide as 10-day monotherapy in HIV-1-positive adults. *J Acquir Immune Defic Syndr*. 2013;63:449-455.
5. Tourret J, Deray G, Isnard-Bagnis C. Tenofovir effect on the kidneys of HIV-infected patients: a double-edged sword? *J Am Soc Nephrol*. 2013;24:1519-1527.
6. Scherzer R, Estrella M, Li Y, et al. Association of Tenofovir Exposure with kidney disease risk in HIV infection. *Aids*. 2012;26:867-875.
7. Cooper RD, Wiebe N, Smith N, Keiser P, Naicker S, Tonelli M. Systematic review and meta-analysis: renal safety of tenofovir disoproxil fumarate in HIV-infected patients. *Clin Infect Dis*. 2010;51:496-505.
8. Ray AS, Cihlar T, Robinson KL, et al. Mechanism of active renal tubular efflux of Tenofovir. *Antimicrob Agents Chemother*. 2006;50:3297-3304.
9. Atta MG, De Seigneux S, Lucas GM. Clinical pharmacology in HIV therapy. *Clin J Am Soc Nephrol*. 2019;14:435-444.
10. Venter WDF, Moorhouse M, Sokhela S, et al. Dolutegravir plus two different prodrugs of Tenofovir to treat HIV. *N Engl J Med*. 2019;381:803-815.
11. Keizer RJ, Karlsson MO, Hooker A. Modeling and simulation workbench for NONMEM: tutorial on Pirana, PsN, and Xpose. *CPT Pharmacometrics Syst Pharmacol*. 2013;2:e50.
12. Savic RM, Jonker DM, Kerbusch T, Karlsson MO. Implementation of a transit compartment model for describing drug absorption in pharmacokinetic studies. *J Pharmacokinet Pharmacodyn*. 2007;34:711-726.
13. Janmahasatian S, Duffull SB, Ash S, Ward LC, Byrne NM, Green B. Quantification of lean bodyweight. *Clin Pharmacokinet*. 2005;44:1051-1065.
14. Anderson BJ, Holford NHG. Mechanism-based concepts of size and maturity in pharmacokinetics. *Annu Rev Pharmacol Toxicol*. 2008;48:303-332.
15. Dosne A-G, Bergstrand M, Harling K, Karlsson MO. Improving the estimation of parameter uncertainty distributions in nonlinear mixed effects models using sampling importance resampling. *J Pharmacokinet Pharmacodyn*. 2016;43:583-596.
16. Jackson A, Moyle G, Watson V, et al. Tenofovir, emtricitabine intracellular and plasma, and efavirenz plasma concentration decay following drug intake cessation: implications for HIV treatment and prevention. *J Acquir Immune Defic Syndr*. 2013;62:275-281.
17. Jullien V, Tréluyer JM, Rey E, et al. Population pharmacokinetics of tenofovir in human immunodeficiency virus-infected patients taking highly active antiretroviral therapy. *Antimicrob Agents Chemother*. 2005;49:3361-3366.
18. Lu Y, Goti V, Chaturvedula A, et al. Population pharmacokinetics of Tenofovir in HIV-1-uninfected members of Serodiscordant couples and effect of dose reporting methods. *Antimicrob Agents Chemother*. 2016;60:5379-5386.
19. Eke AC, Shoji K, Best BM, et al. Population pharmacokinetics of tenofovir in pregnant and postpartum women using tenofovir disoproxil fumarate. *Antimicrob Agents Chemother*. 2021;65:e02168-20.
20. Dumond JB, Nicol MR, Kendrick RN, et al. Pharmacokinetic modelling of Efavirenz, Atazanavir, lamivudine and Tenofovir in the female genital tract of HIV-infected pre-menopausal women. *Clin Pharmacokinet*. 2012;51:809-822.
21. Valade E, Bouazza N, Lui G, et al. Population pharmacokinetic modeling of tenofovir in the genital tract of male HIV-infected patients. *Antimicrob Agents Chemother*. 2017;61:e02062-16.
22. Collins JW, Heyward Hull J, Dumond JB. Comparison of tenofovir plasma and tissue exposure using a population pharmacokinetic model and bootstrap: a simulation study from observed data. *J Pharmacokinet Pharmacodyn*. 2017;44:631-640.
23. Tanaudommongkon A, Chaturvedula A, Hendrix CW, et al. Population pharmacokinetics of tenofovir, emtricitabine and intracellular metabolites in transgender women. *Br J Clin Pharmacol*. 2022;88:3674-3682.
24. Greene SA, Chen J, Prince HMA, et al. Population modeling highlights drug disposition differences between Tenofovir Alafenamide and Tenofovir Disoproxil Fumarate in the blood and semen. *Clin Pharmacol Ther*. 2019;106:821-830.
25. Lee WA, He GX, Eisenberg E, et al. Selective intracellular activation of a novel prodrug of the human immunodeficiency virus reverse transcriptase inhibitor tenofovir leads to preferential distribution and accumulation in lymphatic tissue. *Antimicrob Agents Chemother*. 2005;49:1898-1906.
26. Gagnieu MC, Barkil ME, Livrozet JM, et al. Population pharmacokinetics of Tenofovir in AIDS patients. *J Clin Pharmacol*. 2008;48:1282-1288.
27. Burns RN, Hendrix CW, Chaturvedula A. Population pharmacokinetics of tenofovir and tenofovir-diphosphate in healthy women. *J Clin Pharmacol*. 2015;55:629-638.

28. Baheti G, Kiser JJ, Havens PL, Fletcher C. V plasma and intracellular population pharmacokinetic analysis of Tenofovir in HIV-1-infected patients †. *Antimicrob Agents Chemother*. 2011;55:5294-5299.
29. Parant F, Miailhes P, Brunel F, Gagnieu MC. Dolutegravir population pharmacokinetics in a real-life cohort of people living with HIV infection: a covariate analysis. *Ther Drug Monit*. 2019;41:444-451.
30. Thurman AR, Schwartz JL, Cottrell ML, et al. Safety and pharmacokinetics of a Tenofovir Alafenamide Fumarate-Emtricitabine based Oral antiretroviral regimen for prevention of HIV Acquisition in Women: a randomized controlled trial. *EClinicalMedicine*. 2021;36:100893.
31. Begley R, das M, Zhong L, Ling J, Kearney BP, Custodio JM. Pharmacokinetics of Tenofovir Alafenamide when Coadministered with other HIV antiretrovirals. *J Acquir Immune Defic Syndr*. 2018;78:465-472.

SUPPORTING INFORMATION

Additional supporting information can be found online in the Supporting Information section at the end of this article.

How to cite this article: Kawuma AN, Wasmann RE, Sinxadi P, et al. Population pharmacokinetics of tenofovir given as either tenofovir disoproxil fumarate or tenofovir alafenamide in an African population. *CPT Pharmacometrics Syst Pharmacol*. 2023;12:821-830. doi:10.1002/psp4.12955